

From an Interior Point to a Corner Point: Smart Crossover

Dongdong Ge

Research Institute for Interdisciplinary Sciences, Shanghai University of Finance and Economics, Shanghai, 200433, China.
ge.dongdong@shufe.edu.cn

Chengwenjian Wang

Department of Mathematics, ETH Zurich, Zurich, 8051, Switzerland. wchengwenjia@student.ethz.ch

Zikai Xiong

MIT Operations Research Center, Cambridge, MA 02139, USA. zikai@mit.edu

Yinyu Ye

Department of Management Science and Engineering, Stanford University, Stanford, CA 94305, USA. yyye@stanford.edu

Identifying the optimal basic feasible solutions of linear programming problems is critical for mixed integer programming, and the crossover is the procedure to recover an optimal corner/extreme point from a suboptimal solution (the output of first-order methods) or the relative interior of the optimal face (the output of interior point methods). Unfortunately, this procedure in linear programming, compared with the previous stage of obtaining nearly optimal solutions, frequently turns out to be the actual computation bottleneck in practical applications. Our work shows that this bottleneck can be resolved if smartly taking advantage of problem characteristics and implementing customized strategies. Among the important linear programming problems, many of them arise from network applications and exhibit network structure. We look to the tree structure of the optimal solutions and propose a tree-based crossover algorithm, aimed at recovering basic solutions via identifying nearby spanning tree structures. For other general linear programming problems, we propose an approach to recover the optimal basic solution via moving from the relative interior of the optimal face to an extreme point. Computational experiments show the significant speed-ups of our methods over state-of-art commercial solvers on classical linear programming problem benchmarks, network flow problem benchmarks, and MINST datasets.

Key words: linear programming; optimal transport; network flow problem; first-order method, interior point method

1. Introduction.

As one of the most fundamental problems in operation research, linear programming (LP) is an essential tool in a wide range of practical applications, such as transportation, scheduling, inventory control, revenue management, see Bowman (1956), Charnes and Cooper (1954), Hanssmann and Hess (1960), Liu and Van Ryzin (2008). In LP problems, *basic feasible solution* (BFS) is also equivalent to *vertex solution*, *corner solution* or *extreme point* of the feasible set. In many LP applications, BFS is essentially important for many reasons. First,

BFS is necessary for the warm start of the simplex method, which cannot start from a non-corner solution given by the interior point method or first-order methods. Second, BFS promotes special structure of the problem, such as sparsity, which is valuable in business decision making and the subproblems of some discrete optimization problems. Moreover, for mixed integer programming, obtaining the optimal BFS of the LP relaxation subproblems is critical for promoting integral solutions. Furthermore, the optimal BFS of LP is already integral for some problems, such as network flow problems with integral parameters, in which the incidence matrix has the *total unimodularity* property and thus when the problem parameter is integral, an optimal BFS of its LP relaxation is already an optimal integer solution.

Simplex methods and interior point methods are the two traditional LP algorithms, and both of them have led the advances of operations research since decades ago. The simplex method went through basic solutions so the output is essentially already an optimal BFS. However, it is not a polynomial time algorithm and could heavily suffer from the problem scale, see Klee and Minty (1972). On the other hand, compared with the simplex method, although the interior point method often converges faster in practice for larger applications but only returns an interior point solution instead of a BFS. To deal with it, the crossover is the procedure to obtain an optimal BFS from an interior point solution. Traditionally, it starts from an optimal primal-dual solution via the interior point method and then pushes the relatively interior point towards the corner points by doing simplex-like iterations, see Mitra et al. (1988) and Kortanek and Jishan (1988). Unfortunately, in many LP cases especially the recently emerged large-scale LP applications, its computation time often largely exceeds that of the interior point method because it spent tremendous time on the simplex-like iterations or even fails because of the huge problem scale. The same dilemma happens to first-order methods, which is usually only able to obtain approximate solutions due to the lack of speed when converging to highly-accurate solutions, see Lin et al. (2020b), Liu et al. (2022), Applegate et al. (2021b,a), O'donoghue et al. (2016), Li et al. (2020) for examples of general-purpose LP algorithms, and Cuturi (2013), Yang et al. (2021), Ge et al. (2019), Altschuler et al. (2017), Gao et al. (2021) for examples of problem-focused first-order LP algorithms. However, considering that these problems usually have unique characteristics, if we can utilize those characteristics and adopt ad-hoc crossover strategies smartly, the performance of LP solvers can be considerably improved.

There have been significant efforts devoted to identify the optimal basis from the given interior point solution since decades ago. For example, Mitra et al. (1988) and Kortanek and Jishan (1988) develop an algorithm called purification that implements simplex-like iterations to push the nonbasic variable with intermediate values to the lower or upper bound. Megiddo (1991) proposes an algorithm to find an optimal basis from an optimal primal-dual solution. Bixby and Saltzman (1994) slightly modify this algorithm, simultaneously maintaining non-negativity in each pivot, and iterating towards complementarity. Andersen and Ye (1996) combine the work of Megiddo (1991) and Ye (1992), constructing an approximate problem with a known BFS, and proving that the optimal basis remains unchanged if starting from a high-accuracy solution. Further research (Andersen 1999) suggests some modifications to exploit problem structure and enhance computational efficiency. These papers from decades ago mainly discuss a quite ideal situation — basis identification procedure starting from a primal-dual optimal solution pair, but none of them focus on inexact or low-precision solution, which could be derived more efficiently in practice by recently emerged LP algorithms now. Only few research in recent years attempt to study this problem. Very limited examples include Galabova and Hall (2020), who reveals that the open source solver Clp¹ implements the 'Idiot' crash to increase the sparsity of the given solution via a penalty method.

Nowadays, the traditional interior point method is usually no longer applicable for many huge scale LP problems due to its high per iteration cost. One path of research is to simplify the computation by applying first order methods on the subproblems and exploiting the problem structure. For instance, instead of applying Newton's method, Lin et al. (2020b) propose an ADMM-Based Interior Point Method (ABIP), which avoids multiple matrix factorizations by using alternating direction method of multipliers (ADMM) to minimize the barrier function of primal-dual path-following formulation for LP. Liu et al. (2022) present a primal-dual majorization-minimization method which also requires only one matrix factorization, and prove the globally linearly convergence. For special LP applications. Applegate et al. (2021a) avoid any matrix factorization by directly using primal-dual hybrid gradients with adaptive restarts on the original LP problem. For some important large-scale problems, many researchers develop approximate methods that fully exploit the problem's

¹<https://github.com/coin-or/Clp>

unique structure, especially the network structure, e.g. *optimal transport problem* (Cuturi 2013, Altschuler et al. 2017, Lin et al. 2019) and *Wasserstein barycenter problem* (Benamou et al. 2015, Janati et al. 2020, Lin et al. 2020a, Ge et al. 2019). However, the state-of-the-art commercial LP solvers still cannot benefit from these emerging first-order solutions because those solutions are usually of low accuracy and lack the corresponding dual solution.

As an important case of LP, the *minimum cost flow* (MCF) problem has an noteworthy property: its incidence matrix is *totally unimodular*, which means when all parameters are integral, each basic solution is also integer-valued. So once any extreme point on the optimal face is accessible, solving the LP relaxation with total unimodularity property is already enough for mixed integer programming. It should also be mentioned that the network simplex method has been well developed to obtain the optimal BFS of MCF problems (Dantzig 1963, Ahuja et al. 1993). But for those problems at a huge scale, the network simplex method cannot be efficiently parallelized and there's still no efficient algorithm developed yet, compared with general first-order methods like ABIP (Lin et al. 2020b) or other methods for its special cases, like the auction algorithm (Bertsekas and Castanon 1989) and the Sinkhorn method (Cuturi 2013).

Besides, MCF problems include many important special cases, and the optimal transport problem is one of them. Wagner (1959) has proven that MCF problems can be equivalently transformed into optimal transport problems. Besides, optimal transport problems have served as a fundamental for a wide range of fields, including mathematics (Villani 2003, Santambrogio 2015), economics (Galichon 2018)) and machine learning (Nguyen 2013, Ho et al. 2019). The recent large-scale applications placed significant new demands on the calculation efficiency of optimal transport problems. Due to the usage of entropy regularization, Sinkhorn method (Cuturi 2013) has significantly lowered the complexity and triggers a series of research (Genevay et al. 2016, Altschuler et al. 2017, Dvurechensky et al. 2018, Jambulapati et al. 2019), but an unignorable drawback of these methods is that they cannot obtain either an exact optimal point, or even a BFS.

There are also many other important LP problems that contain network structure, such as the Wasserstein barycenter problem. The Wasserstein barycenter problem has a similar structure with optimal transport problems but is computationally harder, and Lin et al. (2020a) has proven that general fixed-support Wasserstein barycenter problems are not MCF problems. In the last two decades, the Wasserstein barycenter problem has become

particularly increasingly important in many areas, such as physics (Buttazzo et al. 2012, Cotar et al. 2013), economics (Carlier and Ekeland 2010), and machine learning (Cuturi and Doucet 2014). Many efforts have been devoted to develop fast algorithms for the Wasserstein barycenter problem via entropy regularization or matrix structure, e.g. Cuturi and Doucet (2014), Kroshnin et al. (2019), Janati et al. (2020), Ge et al. (2019) but all of these methods cannot identify bases.

For problems with network structure, such as optimal transport problem, Wasserstein barycenter problems (with fixed support), and the general MCF problem, our smart crossover can start from an approximate solution returned by these algorithms and identify a nearby basis.

Contribution. In this paper, we consider problems in the following standard form:

$$\min_{x \in \mathbb{R}^n} c^\top x \quad \text{s. t. } Ax = b, x \geq 0, \quad (1)$$

where $A \in \mathbb{R}^{m \times n}$, $c \in \mathbb{R}^n$ and $b \in \mathbb{R}^m$. Given any primal solution \tilde{x} , such as outputs of interior point methods or any low-accuracy first-order method, the crossover procedure warmly starts the simplex method and iterates to an optimal BFS of (1). Generally, the crossover procedure consists of two phases, *basis identification* and *reoptimization*. In the basis identification phase, the algorithm can identify a BFS near \tilde{x} . In the reoptimization phase, it applies simplex-like iterations to obtain an optimal BFS.

- For large scale LP problems with network structure, given any approximate solution \tilde{x} , we propose a criterion to evaluate the possibility of each column being in the optimal basis and a column generation based basis identification phase to reach a nearby basis, without utilizing any information from the dual solution. Besides, based on the spanning tree characteristics of BFS, we develop a spanning tree structure based basis identification method. We also design a reoptimization phase to iterate towards the optimal corner point.

- Experiments of MCF problems are conducted in public network flow datasets, and the optimal transport problems and Wasserstein barycenter problems are tested on MNIST dataset. The results show that the crossover can largely promote sparsity in final solutions. Compared with commercial solvers' crossover, our crossover method exhibits very significant speed-ups. Furthermore, we also present how the combination of first-order methods, such as Sinkhorn algorithm, and our crossover method, has huge advantages over other algorithms in practice.

- For general LP problems with long crossover computation time, it is the high dimension of the optimal face that causes the high basis identification cost from the simplex-like reoptimization iterations. For these problems, we propose a perturbation crossover that can firstly construct an approximate optimal face via the primal dual solution pair, and then directly find a corner solution in the optimal face. Experiments on LP benchmark problems show that our crossover method, as an alternative crossover approach, can significantly improve commercial solvers' crossover performance for the problems difficult for current state-of-art solvers.

Our paper studies the crossover from a low-precision solution to a corner solution, especially for the problems with network flow structure. This powerful technique of the perturbation crossover method has also been used on the rapid-growing commercial optimizer COPT, leading to a breakthrough from its version 1.5 to 1.6.

Organizations. The rest of the paper is organized as follows. In Section 2, we introduce some preliminaries and backgrounds. In Section 3, we propose a network structure based two-phase crossover method for MCF problems and general LP problems. In Section 4, we propose an perturbation crossover method to accelerate the crossover procedure in general-purpose LP solvers. The computational results are presented in Section 5.

Notations. We let $[n]$ be the shorthand for $\{1, 2, \dots, n\}$. For a set \mathcal{X} , the notation $|\mathcal{X}|$ denotes the cardinality of \mathcal{X} . For $\mathcal{X} \subset [n]$ and vector $u \in \mathbb{R}^n$, $u_{\mathcal{X}}$ is the $|\mathcal{X}|$ -vector constituted by the components of u with indices in \mathcal{X} . 1_n and 0_n are the n -dimensional vector of ones and zeros. For a matrix X and scalar x , $X \geq x$ means each component of X is greater than or equal to x . For a matrix $A = (A)_{ij}$, the positive part and negative part of A are A^+ and A^- , $(A^+)_{ij} := \max\{(A)_{ij}, 0\}$, and $(A^-)_{ij} := \max\{-(A)_{ij}, 0\}$. A_i , A_j and A_{ij} denote the i -th row, j -th column and the component in the i -th row and the j -th column. For a graph $(\mathcal{N}, \mathcal{A})$ and $i \in \mathcal{N}$, $O(i), I(i)$ denote the node sets connecting to i , specifically, $O(i) := \{j \mid (i, j) \in \mathcal{A}\}$, $I(i) := \{j \mid (j, i) \in \mathcal{A}\}$. And for any two sets \mathcal{X} and \mathcal{Y} , we use $\mathcal{X} \setminus \mathcal{Y}$ to denote $\{x \mid x \in \mathcal{X} \text{ but } x \notin \mathcal{Y}\}$.

2. Preliminary.

LP problems with network structure. Among the current large-scale LP real-world applications, many of them have network structure. The optimal transport problem is a typical one which is also a special equivalent form of the MCF problem. The formulation of optimal transport problems is as follows:

EXAMPLE 1 (OPTIMAL TRANSPORT PROBLEM). There is a directed graph $\mathcal{G} = (\mathcal{N}, \mathcal{A})$ with cost c_{ij} per unit of flow for each arc $(i, j) \in \mathcal{A}$. The nodes \mathcal{N} can be divided into two groups, suppliers \mathcal{S} and consumers \mathcal{C} . And arcs \mathcal{A} pairwise connect consumers and suppliers, in the direction from the former to the latter, i.e., $\mathcal{A} = \mathcal{S} \times \mathcal{C} := \{(i, j) : i \in \mathcal{S}, j \in \mathcal{C}\}$. For any $i \in \mathcal{S}$, $O(i) = \mathcal{C}$ and $I(i) = \emptyset$, while for any $j \in \mathcal{C}$, $O(j) = \emptyset$ and $I(j) = \mathcal{S}$. For any supplier i and consumer j , s_i and d_j respectively denote the capacity of the supply and demand. Besides, the capacity of any route is unlimited. Then an optimal transport problem can be rewritten as follows:

$$\begin{aligned}
& \min_f \sum_{(i,j) \in \mathcal{S} \times \mathcal{C}} c_{ij} f_{ij} \\
& \text{s. t. } \sum_{j \in \mathcal{C}} f_{ij} = s_i, \quad \forall i \in \mathcal{S} \\
& \quad \sum_{i \in \mathcal{S}} f_{ij} = d_j, \quad \forall j \in \mathcal{C} \\
& \quad f_{ij} \geq 0, \quad \forall (i, j) \in \mathcal{S} \times \mathcal{C}
\end{aligned} \tag{2}$$

There are also many other important problems that origin from network structure, such as the Wasserstein Barycenter problems with fixed support.

EXAMPLE 2 (FIXED-SUPPORT WASSERSTEIN BARYCENTER PROBLEM). The Wasserstein barycenter of probability measures $(\mu_k)_{k=1}^N$ is defined as the probability measure μ_0 with the minimal sum of Wasserstein distance to each probability measure. For the convenience of computation, we usually assume that $(\mu_k)_{k=1}^n$ are discrete probability measures, with support points $\{x_i^k\}_{i \in [m_k]}$ and weight μ^k , where $\mu^k \in \mathbb{R}^{m_k}$. Similarly, in Wasserstein barycenter problems, the support points of the barycenter $\{\hat{x}_i\}_{i \in [m]}$ are also fixed, but the weight μ is part of the variables. Then the Wasserstein barycenter between $\{\mu_k\}_{k=1}^N$ can be represented by the following problem:

$$\begin{aligned}
& \min_{\mu, \{X_k\}_{k \in [N]}} \sum_{k=1}^N \langle C_k, X_k \rangle \\
& \text{s. t. } X_k \mathbf{1}_m = \mu^k, X_k \geq 0, \text{ for all } k \in [N] \\
& \quad X_k^\top \mathbf{1}_{m_k} = \mu, \text{ for all } k \in [N] \\
& \quad \mu \geq 0, X_k \geq 0, \text{ for all } k \in [N]
\end{aligned} \tag{3}$$

where $\{X_k\}_{k=1}^N$ represents the transportation plans between the barycenter and the N probability measure, and $\{C_k\}_{k=1}^N$ denotes the cost matrices.

The Wasserstein barycenter problem has similar structure with the optimal transport problem but is significantly harder. If we fix the weight of the barycenter u , then the fixed-support Wasserstein Barycenter problem is equivalent to N separate optimal transport problems. But Lin et al. (2020a) has already proven that most Wasserstein barycenter problems are not MCF problems.

Optimal face. For the general primal linear program (1), the corresponding dual problem is

$$\max_{y,s} b^\top y \quad \text{s.t.} \quad A^\top y + s = c, \quad s \geq 0 \quad (4)$$

There exists at least one pair of optimal solution pair (x^*, s^*) strictly complementary (Goldman and Tucker 1956), i.e.,

$$\mathcal{P}(x^*) \cap \mathcal{P}(s^*) = \emptyset, \quad \mathcal{P}(x^*) \cup \mathcal{P}(s^*) = [n]. \quad (5)$$

where $\mathcal{P}(x) := \{i : x_i > 0\}$. Moreover, if we denote \mathcal{P}^* as $\mathcal{P}(x^*)$, and denote $\bar{\mathcal{P}}^*$ as $\mathcal{P}(s^*)$, then $\{\mathcal{P}^*, \bar{\mathcal{P}}^*\}$ is called the *optimal partition*. One can further prove that for any other complementary solution pair (x, s) ,

$$\mathcal{P}(x) \subseteq \mathcal{P}^*, \quad \mathcal{P}(s) \subseteq \bar{\mathcal{P}}^*. \quad (6)$$

Therefore, the optimal face of the primal problem (1) can be written as

$$\Theta_p := \{x : Ax = b, \quad x \geq 0, \text{ and } x_{\bar{\mathcal{P}}^*} = 0\}, \quad (7)$$

and the optimal face of the dual problem (4) is

$$\Theta_d := \{(y, s) : A^\top y + s = c, \quad s \geq 0, \text{ and } s_{\mathcal{P}^*} = 0\}. \quad (8)$$

Mehrotra and Ye (1993) have proven that the interior point method will always converge to the relative interior of the optimal face. Therefore, when the cardinality of \mathcal{P}^* is very large and the dimension of the optimal face is high, it will be increasingly difficult to identify an optimal BFS in the optimal face. Usually in real LP applications, the optimal solution is highly degenerate and the cardinality of \mathcal{P}^* is huge, so the crossover often becomes the bottleneck.

Column generation method. The column generation method is an efficient approach for large scale LP problems. Instead of directly solving the original problem (1), the column generation method is essentially a sequence of master iterations. In each iteration, we form a collection of columns A_i , $i \in \Lambda$, and solve the following restricted problem $LP(\Lambda)$:

$$\min_x \sum_{i \in \Lambda} c_i x_i \quad \text{s. t.} \quad \sum_{i \in \Lambda} A_i x_i = b, \quad x_{[n] \setminus \Lambda} = 0, \quad x \geq 0. \quad (9)$$

See algorithm 1 for the general framework. The collection Λ_{k+1} contains the basis of the solution x^k from $LP(\Lambda_k)$ so $LP(\Lambda_{k+1})$ can easily start from x^k . The sequence $(\Lambda_k)_k$ can be generated by

$$\Lambda_{k+1} \leftarrow \Lambda_k \cup \arg \min_i \{\bar{c}_i \mid i \notin \Lambda_k\} \quad (10)$$

in each iteration, where \bar{c}_i is the reduced cost of the solution of $LP(\Lambda_k)$ in problem (1), i.e. $\bar{c}_i = c_i - c_{B_k}^\top B_k^{-1} A_i$ and B_k is the optimal basis of $LP(\Lambda_k)$. See Bertsimas and Tsitsiklis (1997) for more variants.

Algorithm 1 General Column Generation Method

- 1: Initialize iteration counter $k = 1$.
 - 2: **while** the reduced cost $\bar{c} \not\leq 0$ **do**
 - 3: **Solve the restricted problem:** Use the simplex method to solve $LP(\Lambda_k)$ and obtain an optimal basis B_k .
 - 4: **Check optimality:** Update reduced cost $\bar{c} \leftarrow c - c_{B_k}^\top B_k^{-1} A$, and $k \leftarrow k + 1$.
 - 5: **end while**
-

3. Network Crossover Method.

In this section, we consider the general minimum cost flow problems (11) defined below.

DEFINITION 1 (MINIMUM COST FLOW (MCF) PROBLEM). There is a directed graph $\mathcal{G} = (\mathcal{N}, \mathcal{A})$ with capacity u_{ij} and cost c_{ij} per unit of flow for each arc $(i, j) \in \mathcal{A}$. Among them, u_{ij} must be non-negative and even possibly infinite. And b_i represents the external supply or demand for each node $i \in \mathcal{N}$. If we use f_{ij} to denote the amount of flow on arc (i, j) , a general minimum cost flow problem can be formulated as follows,

$$\begin{aligned} \min_f \quad & \sum_{(i,j) \in \mathcal{A}} c_{ij} f_{ij} \\ \text{s. t.} \quad & b_i + \sum_{j \in \mathcal{I}(i)} f_{ji} = \sum_{j \in \mathcal{O}(i)} f_{ij}, \quad \forall i \in \mathcal{N} \\ & 0 \leq f_{ij} \leq u_{ij}, \quad \forall (i, j) \in \mathcal{A}, \end{aligned} \quad (11)$$

where $\mathcal{O}(i) := \{j : (i, j) \in \mathcal{A}\}$, $\mathcal{I}(i) := \{j : (j, i) \in \mathcal{A}\}$.

Suppose that we have already got an approximate solution \tilde{f} of the problem (11) via interior point method (which can be extended to or any first-order method variants), now we have the following lemma:

LEMMA 1. *For the general MCF problem (11), named $MCF(b, c, u)$, let $(\mathcal{L}, \mathcal{U})$ be an arbitrary partition of \mathcal{A} , then we can construct an equivalent problem $MCF(\bar{b}, \bar{c}, \bar{u})$ such that if \bar{f}^* is an optimal solution of $MCF(\bar{b}, \bar{c}, \bar{u})$, then*

$$\tilde{f}_{ij}^* := \begin{cases} \bar{f}_{ij}^*, & \text{for } (i, j) \in \mathcal{L} \\ u_{ij} - \bar{f}_{ij}^*, & \text{for } (i, j) \in \mathcal{U} \end{cases} \quad (12)$$

is an optimal solution of $MCF(b, c, u)$, vice versa.

See appendix for the proof of it. Since the iterations of the interior point method converge to an interior point of the optimal face, if the solution \tilde{f} is of enough accuracy then the partition $\mathcal{L} := \{(i, j) : 0 \leq f_{ij} \leq u_{ij}/2\}$ and $\mathcal{U} := \mathcal{A} \setminus \mathcal{L}$ will keep the same in the rest iterations. Moreover, under this accuracy assumption, when the problem has a unique optimal solution, the original MCF problem is directly equivalent to the incapacitated version of $MCF(\bar{b}, \bar{c}, \bar{u})$. Without loss of generality, now we assume that $0 \leq \tilde{f}_{ij} \leq u_{ij}/2$ for each arc $(i, j) \in \mathcal{A}$.

In incapacitated MCF problems, the basic solutions have an important property: a solution f is a basic (feasible) solution if and only if it is a (feasible) *tree solution* (Ahuja et al. 1993). Generally speaking, the tree solutions in the incapacitated MCF problems are those whose nonzero components can form a spanning tree, without considering the direction of flows (Ahuja et al. 1993). Therefore, for a nondegenerate BFS of the incapacitated MCF problem in a connected graph, there are exactly $|\mathcal{N}| - 1$ strictly positive components, connecting each node in the graph and corresponding to a spanning tree in \mathcal{G} . However, for an interior point solution, the flow in each arc is strictly positive, so the arc that serves the most flow to a single node has higher potential and priority of being in the basis than other flows. We use the following *flow ratio* to measure it.

DEFINITION 2 (FLOW RATIO FOR MCF PROBLEM). For any flow f , we define maximal flow on node k : $f^k := \sum_{l \in \mathcal{O}(k)} f_{kl} + \sum_{l \in \mathcal{I}(k)} f_{lk}$. And then the flow ratio of the arc is defined as $r_{ij} := \max\{f_{ij}/f^i, f_{ij}/f^j\}$.

One can easily observe that the flow ratio measures the proportion that the flow in a specific arc serves in all the conjoint arcs. Since the iterations of the interior point method will converge to relative interior of the optimal face, so for the arcs not in the optimal face, the flow ratio gradually converges to zero. The flow ratio contains not only the magnitude information but also the graph information, so the flow ratio is more powerful than the criterion proposed by Mehrotra and Ye (1993) in predicting the primal optimal face \mathcal{P}^* . The arc/column with a higher flow ratio is more likely to be in the basis, so given any approximate solution \tilde{f} we can sort these arcs as $s := (s_1, s_2, \dots, s_{|\mathcal{N}|})$, in which the first $|\mathcal{N}|$ arcs connect all nodes with the largest ratio flow and the rest array is arranged in descending order of \tilde{f} 's flow ratio.

Now we propose the following column generation based crossover method, composed of two phases, basis identification and reoptimization.

Column generation basis identification (COL-BI). The basis identification phase is aimed at capturing a nearby BFS of the non-corner solution \tilde{f} . The key idea in the basis identification phase is to follow the potentials to implement the column generation algorithm 1 on an equivalent problem and get a nearby BFS of the original problem, so we call this phase Col-BI for "Column generation basis identification".

For any general LP problem (1) with upper bounds of x , we can use the *big-M method* to form the following equivalent problem

$$\begin{aligned} \min_{x_0, x_a} \quad & c^\top x_0 + M \mathbf{1}_m^\top x_a \\ \text{s. t.} \quad & Ax_0 + Ix_a = b \\ & l \leq x_0 \leq u, x_a \geq 0 \end{aligned} \tag{13}$$

where I is an identity matrix in $\mathbb{R}^{m \times m}$, and M is an large positive scalar. So there is an obvious basic feasible solution x , $x^\top := (x_0^\top \ x_a^\top) = (0_n^\top \ b^\top)$, that can serve as the starting point the simplex method in the column generation method. Besides, if the original problem is the general MCF problem (11), once M is larger than $n * \max_j |c_j|$, the problem (13) is equivalent to the original problem. Then we directly adopt algorithm 1, in which $\Lambda_0 := \{n+1, \dots, n+m\}$ and the sequential sets of indices $(\Lambda_k)_k$ are generated by

$$\Lambda_{k+1} \leftarrow (\Lambda_k \cup \{i_{s_1}, i_{s_2}, \dots, i_{s_{\theta_k}}\}) \setminus \{n+1 \leq i \leq n+m : x_i^k \text{ is nonbasic}\}. \tag{14}$$

Here $(\theta_k)_k$ can be any monotonously increasing integer series, such as $\theta_k = 2^k$, and the i_j is the index of the column in the LP formulation corresponding to the j -th arc in the graph.

When all the artificial variables of x^k are nonbasic, $x_{1:n}^k$ is a BFS for the original problem. If our goal is to obtain a BFS but don't require it to be exactly optimal, the $x_{1:n}^k$ is a BFS close enough to the optimal solutions.

Reoptimization. After obtaining an advanced starting BFS of the original problem, we can continue to implement the reoptimization phase to obtain an ε -optimal corner solution (the reduced cost $\bar{c} \geq -\varepsilon$). In this phase, we use the column generation algorithm 1 on the original problem and generate the sequence $(\Lambda_k)_k$ by

$$\Lambda_{k+1} \leftarrow \Lambda_k \cup \{i : \bar{c}_i < -\varepsilon\} \cup \{s_1, s_2, \dots, s_{\theta_k}\} \quad (15)$$

until $\bar{c} \geq -\varepsilon$. Similarly, $(\theta_k)_k$ can be any monotonously increasing integer series.

Spanning tree basis identification (TREE-BI). In addition to the general COL-BI, we also have an alternative basis identification method for MCF problems. Because the BFS of any MCF problem must be a feasible tree solution, and a tree solution corresponds to a spanning tree in the graph. Therefore, instead of directly dealing with the LP problem, we can alternatively try to construct the spanning tree with the highest sum of flow ratio in the graph. If the given non-corner solution is of enough high accuracy and the optimal solution is unique, such a spanning tree can exactly corresponds to the optimal BFS. If not, we can also obtain a high-quality basic solution in a very short time. Besides, many efforts have been devoted to design the algorithm to find the maximum/minimum weight spanning tree. For the classic algorithms with complexity $\mathcal{O}(|\mathcal{A}| \log(|\mathcal{N}|))$, there are Prim's algorithm (Prim 1957, Dijkstra et al. 1959) and Kruskal's algorithm (Kruskal 1956). For faster almost linear time algorithms, see (Karger et al. 1995, Chazelle 2000). When the accuracy of the non-corner solution is not high enough and the tree solution is infeasible, we can also further implement network-simplex-like iterations to push it to the feasible set.

Among the problems with network structure, for optimal transport problems, the network simplex iterations can be especially simple. We have the following lemma:

LEMMA 2. *For an optimal transport problem, suppose that the flow f is infeasible, with $f_{ij} < 0, (i, j) \in \mathcal{A}$. Then there exist $j', i' \in \mathcal{N}$ such that $f_{ij'} > 0, f_{i'j} > 0$ and $(i', j') \in \mathcal{A}$.*

Proof. Since $(i, j) \in \mathcal{A}$, we have $i \in \mathcal{S}$ and $j \in \mathcal{C}$. Besides, we have $\sum_{l \in \mathcal{C}} f_{il} = s_i \geq 0$ and $\sum_{l \in \mathcal{S}} f_{lj} = d_j \geq 0$. Note that we already have $f_{ij} < 0$ so there must exist $f_{ij'} > 0, j' \in \mathcal{C}$ and $f_{i'j} > 0, i' \in \mathcal{S}$. Because $i' \in \mathcal{S}$ and $j' \in \mathcal{C}$, $(i', j') \in \mathcal{A}$. \square

Thus, by this lemma, the network simplex method can directly eliminate the inverse branch, say $f_{ij} < 0$, by repeating the following process: finding j', i' such that $f_{ij'}, f_{i'j} > 0$ are positive and increasing value in the loop $i \rightarrow j \rightarrow i' \rightarrow j' \rightarrow i$ until one branch of this loop goes to zero. Therefore, the network simplex iteration in the push phase can be directly written as follows:

Algorithm 2 The ‘Push’ Phase for Optimal Transport Problems

- 1: **Input:** a basic solution f and $\Gamma = \{(i, j) \mid f_{ij} < 0\}$
 - 2: **while** Γ is nonempty **do**
 - 3: **for** $(i, j) \in \Gamma$ **do**
 - 4: **Find adjacent positive flows:** $j' \leftarrow \arg \max_{l \in \mathcal{C}} f_{il}$, $i' \leftarrow \arg \max_{k \in \mathcal{S}} f_{kj}$ and let $\theta \leftarrow \min\{-f_{ij}, f_{i'j}, f_{ij'}\}$.
 - 5: **Decrease the negative flow:** $f_{ij} \leftarrow f_{ij} + \theta$, $f_{ij'} \leftarrow f_{ij'} - \theta$, $f_{i'j} \leftarrow f_{i'j} - \theta$, $f_{i'j'} \leftarrow \theta$
 - 6: **end for**
 - 7: Update the set of negative flows $\Gamma \leftarrow \{(i, j) \mid f_{ij} < 0\}$
 - 8: **end while**
-

Extension to other LP problems. For other problems with network structure, the network crossover method can also be easily extended. For instance, although Lin et al. (2020a) prove that Wasserstein barycenter problem is not a special case of MCF problems, it can be separated into many different optimal transport problems if fixing the weight of the barycenter. Using TREE-BI for optimal transport problems, we can still obtain a nearby corner point in a very short time.

For general LP problems, we can also approximately regard them as MCF problems and use column generation based network crossover method. From the view of the graph, there exists an underlying graph $\mathcal{G} := (\mathcal{N}, \mathcal{A})$ in which each column of A corresponds to one arc of the graph. But different from MCF problems, we allow the arcs to connect more than two nodes. Similar to definition 2, now we can also define the general flow ratio for each column of the general LP problem (9):

DEFINITION 3 (FLOW RATIO FOR GENERAL LP PROBLEM). For any non-corner solution x , we define the maximal flow of each row k as $f^k := A_k^+ x + A_k^- x$. Then we can define the flow ratio for each column i as $r_i := \max\{A_{ki} x_i / f^k : k = 1, \dots, m\}$

Intuitively, the flow ratio can similarly measure the highest ratio of the ‘flow’ one column serves among all arcs for each nodes in the approximate graph \mathcal{G} . After that, we sort the columns in descending order of flow ratio, and then follow it with the basis identification phase COL-BI and the reoptimization phase.

4. Perturbation Crossover Method.

The interior point method in commercial LP solvers can usually return a high-accuracy interior point primal dual solution pair (x^k, s^k) for problem (1) but sometimes in real LP applications, the computation time in the crossover procedure can largely exceed that of the interior point method stage, which used to be a significant bottleneck of many application problems for the rapid-growing commercial solver COPT before version 1.6. In this section, we introduce a perturbation crossover method to deal with it.

Mehrotra and Ye (1993) shows that, for a class of classic interior point algorithms, such as Güler and Ye (1993), Kojima et al. (1989) and Ye (1992), one can always get an optimal partition by

$$\mathcal{P}^k := \{j : x_j^k \geq s_j^k\} \text{ or } \mathcal{P}^k := \{j : |x_j^{k+1} - x_j^k|/x_j^k \leq |s_j^{k+1} - s_j^k|/s_j^k\}, \quad (16)$$

but the primal dual pair will always converge to a relative interior point of the optimal face Θ_p and Θ_d . Therefore, when the optimal face contains a huge number of corner points, the traditional crossover procedure often gets stuck in purification.

Since any extreme point in the optimal face is an optimal BFS, our goal is now equivalent to obtaining an extreme point in the optimal face. Using the criterion in (16), we can obtain \mathcal{P}^k , an estimation of \mathcal{P}^* that contains the real \mathcal{P}^* , and the estimated primal optimal face

$$\Theta_p^k := \{x : Ax = b, x \geq 0, \text{ and } x_j = 0 \text{ for } j \in \bar{\mathcal{P}}^k\},$$

where $\mathcal{P}^k \cap \bar{\mathcal{P}}^k = \emptyset$, $\mathcal{P}^k \cup \bar{\mathcal{P}}^k = [n]$. Then we define the perturbed feasibility problem on Θ_p^k :

$$\min_x (c + \varepsilon)^\top x \quad \text{s. t. } x \in \Theta_p^k. \quad (17)$$

Besides, we have the following theorem 1 about the problem (17):

THEOREM 1. *If the optimal face Θ_p for the original problem (1) is bounded and $\mathcal{P}^* \subseteq \mathcal{P}^k$, then there exists a $\delta > 0$, such that for the perturbation ε whose components ε_i are uniformly distributed in $[-\delta, \delta]$ for $i \in \mathcal{P}^k$ and $\varepsilon_i = 0$ for $i \in \bar{\mathcal{P}}$, the perturbed feasibility problem (17) has a unique optimal solution x^* almost surely. Moreover, x^* is an optimal BFS for the original primal problem (1).*

Proof. First of all, since $\mathcal{P}^* \subseteq \mathcal{P}^k$, the optimal face of the perturbed feasibility problem is exactly the same as the optimal face of the original problem Θ_p . Because the optimal face Θ_p is bounded, it should be the convex hull of finite different extreme points $\{v_1, \dots, v_k\}$, and those extreme points of the optimal face are exactly all the optimal basic feasible solution of the problem (1).

Since the feasible set is a polyhedron, the feasible set can be written as:

$$\mathcal{P} := \left\{ \sum_{i=1}^t \lambda_i v_i + \sum_{j=1}^q \theta_j w_j : \sum_{i=1}^t \lambda_i = 1, \lambda_i \geq 0, \theta_j \geq 0 \right\}, \quad (18)$$

where $\{v_i\}$ and $\{w_i\}$ are the extreme points and extreme rays of the feasible set. Let f^* denote the optimal value of problem (1), then $c^\top v_i = f^*$ when $i \leq k$, and $c^\top v_i > f^*$ when $k < i \leq t$, and $c^\top w_j > 0$ for any j .

Therefore, the optimal solution of the perturbed feasibility problem (17) is still the optimal solution of the original problem, if and only if

$$h_1(\varepsilon) := \min_{i \leq k} \varepsilon^\top v_i - \min_{k < i \leq t} (\varepsilon^\top v_i + c^\top v_i - f^*) < 0, \text{ and } h_2(\varepsilon) := (c + \varepsilon)^\top w_i > 0 \text{ for any } i. \quad (19)$$

Since h_1 and h_2 are both continuous functions and (19) holds at the origin, there must exist a neighborhood of the origin, $[-\delta, \delta]^n$, such that for any ε in it, $h_1(\varepsilon) < 0$ and $h_2(\varepsilon) > 0$.

Note that the problem (17) has multiple optimal solutions only if there exists i, j , $1 \leq i < j \leq t$, such that $(c + \varepsilon)^\top (x_i - x_j) = 0$. However, since $x_i \neq x_j$, the set $\{\varepsilon : (x_i - x_j)^\top \varepsilon = (x_i - x_j)^\top c\}$ is of zero Lebesgue measure in \mathbb{R}^n . Besides, there are only finite pairs of extreme points in Θ_p , so the perturbed problem would have a unique optimal solution almost surely if ε uniformly distributed in $[-\delta, \delta]^n$.

□

However, in practice the perturbation is often beyond the theoretical scale and the partition might be suboptimal as well because the practical implementation is more conservative in estimating the partition. Suppose that the practical implementation loosens the criterion for constructing \mathcal{P}^k such that \mathcal{P}^k contains the optimal partition for the following perturbed problem:

$$\min_x (c + \varepsilon)^\top x \quad \text{s. t. } Ax = b, \quad x \geq 0 \quad (20)$$

If this case, we have the following Theorem 2 to estimate the error from perturbation ε :

THEOREM 2. *Let x^k be the solution returned by the interior point method on the original problem (1), with duality gap smaller than δ_g . If the perturbation $\varepsilon \geq 0$, then the optimal basic feasible solution \bar{x}^* of the perturbed problem (17) satisfies:*

$$c^\top \bar{x}^* \leq c^\top x^* + \delta_g + \|\varepsilon\| \|\bar{x}^* - x^k\| , \quad (21)$$

where x^* is the optimal solution of the original LP problem and $\|\cdot\|$ is Euclidean norm.

Proof. Let the corresponding dual variable of x^k be (y^k, s^k) , then the duality gap is $(x^k)^\top s^k \leq \delta_g$. Since the perturbation is positive, $(x^k, y^k, s^k + \varepsilon)$ is a primal dual feasible solution for the perturbed problem (20), with duality gap $(x^k)^\top s^k + (x^k)^\top \varepsilon$.

Now we have

$$c^\top x^k - (s^k)^\top x^k \leq c^\top x^* \leq c^\top x^k, \quad \text{and} \quad (c + \varepsilon)^\top x^k - (s^k + \varepsilon)^\top x^k \leq (c + \varepsilon)^\top \bar{x}^* \leq (c + \varepsilon)^\top x^k ,$$

which means

$$c^\top \bar{x}^* \leq c^\top x^k + \varepsilon^\top x^k - \varepsilon^\top \bar{x}^* \leq c^\top \bar{x}^* \leq c^\top x^* + \delta_g + \|\varepsilon\| \|x^k - \bar{x}^*\| .$$

□

In practice, we can directly adopt crossover procedure starting from \bar{x}^k , the interior point solution of the perturbed feasibility problem, for the original problem, because \bar{x}^k is also an interior point for the original problem. Besides, when solving the problem (17) is not obviously cheaper than solving the problem (20), we can also let \mathcal{P}^k be $[n]$ and use warm starting strategies (Yildirim and Wright 2002, Skajaa et al. 2013) to directly solve the perturbed problem (20). Besides, after obtaining an advanced BFS from the perturbed problem (17) or (20), we can choose to enter the reoptimization phase, if an optimal BFS is required.

5. Numerical Experiments.

In this section, we evaluate our smart crossover methods on classic datasets: benchmark problems for MCF², optimal transport problems generated by MNIST database of handwritten digits³, and LP problems from Hans Mittelmann's benchmarks for optimization

² <https://lemon.cs.elte.hu/trac/lemon/wiki/MinCostFlowData>

³ <http://yann.lecun.com/exdb/mnist/>

software⁴. We run and compare our method with the state-of-the-art solvers: GUROBI (9.0.3), MOSEK (9.2) and CPLEX (Studio129). The experiments are implemented in MATLAB-R2020b and Python 2020.3.5, on a Windows64(x64) computer with processor Intel(R) Core(TM) i7-7820HQ @2.90GHz (4 cores and 8 threads), and 16GB of RAM.

5.1. Network Crossover Method.

In this subsection, we evaluate our network crossover method introduced in Section 3. For convenience of notation, we name the two-phase crossover COL-BI and the reoptimization phase by CNET, and name the two-phase crossover TREE-BI and the reoptimization phase by TNET. The experiments can be divided into two aspects:

- a) testing the crossover procedure separately;
- b) testing the complete solution process, i.e. the time of crossover procedure plus the previous interior point method or first-order method.

Numerical results revealed that, for a), CNET and TNET accelerated the crossover procedure greatly, compared with the commercial solvers in different problem scales and different precision of the initial interior point solution. As for b), in optimal transport problems, our proposed crossover methods together with the low-precision but efficient algorithm SINKHORN (Cuturi 2013) clearly achieve faster results than the traditional network simplex method. This suggests that CNET/TNET truly help make a breakthrough on classic exact algorithms for problems with network structure.

Our main results are carried out on optimal transport problems for the following two considerations. First, optimal transport is a type of fundamental problem with strong, well-studied first-order methods to test the performance of the crossover. Second, it is easier to implement TREE-BI on optimal transport than on general MCF problems and we design TNET for optimal transport accordingly. For experiments a), we use an interior point solution generated by commercial solvers with controllable precision to warm-start the crossover procedure. We conduct experiments with GUROBI, CPLEX, and MOSEK and only present the results with GUROBI due to the similarity of the results. For b), we also include CPLEX's network simplex algorithm.

Also, we perform experiments on MCF problems to further illustrate the applicability of our algorithm. These experiments belong to part a), demonstrating an improvement on

⁴ <http://plato.asu.edu/bench.html>

the crossover procedure. Nevertheless, we believe that similar to optimal transport, the overall promotion of solution over classic benchmarking methods can be reached, with some high-speed first-order methods.

Optimal transport problems generated by MNIST dataset. The MNIST dataset consists of 60,000 images of handwritten digits of size 28 by 28 pixels. We randomly pick two images, normalize the sum of non-zero weights to 1 and create the optimal transport problem of solving the *Wasserstein distance* between them. Figure 1 shows the difference between an approximate solution and corner solutions for a specific generated problem. The solution from the TREE-BI phase is a nearby BFS of the interior point solution. And the solution after reoptimization is the optimal BFS obtained after some simplex iterations. One can easily see that the corner solution is of apparently higher sparsity and fully avoids the biased blurring solution. Meanwhile, the corner solution remains the same shape but largely lowers the dimension.

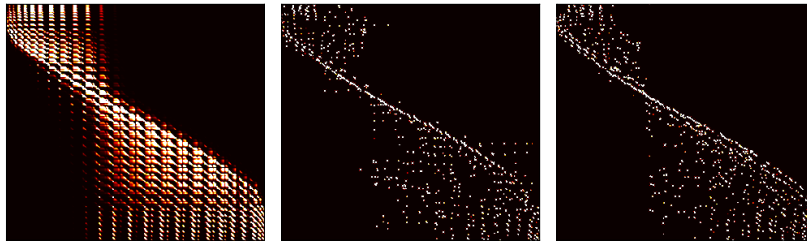


Figure 1 Transport plan of a randomly generated optimal transport problem from MNIST dataset. The left, the middle, and the right are the initial interior point solution, the tree solution from Tree-BI, and the final-solved optimal solution respectively.



Figure 2 The Wasserstein barycenters solved from the interior point method (the first row) and the barycenters after crossover (the second row). Each image is the Wasserstein barycenter of 25 MNIST digit images.

Figure 2 illustrates the difference between the interior point Wasserstein barycenters and the optimal BFS. Note that if fixing the barycenter and applying TREE-BI to construct

the corresponding transportation plan, we can obtain the BFS with the same barycenter shape, so the barycenter after the basis identification phase is the same with the interior point barycenter, but such a BFS is able to be fitted into reoptimization and thus get a high quality suboptimal BFS in a short time. Apparently, the exact barycenter after some simplex iterations from the reoptimization phase is sharper and clearer. This further proves the advantages of a exact/corner solution.

To better exhibit the effect of the problem size, we artificially magnify the images by α ($\alpha = 1, 2, 3, \dots$) times and generate the images with size $28\alpha \times 28\alpha$. We randomly select two images each time, magnifying them and calculating the optimal transport problem between them.

In our experiments, the number of new variables entering the subproblems θ_k in the column generation algorithm is set to be 2^k (see (14), (15)). The regularization coefficient in SINKHORN algorithm (λ in (Cuturi 2013)) is for balancing numerical errors and enhancing accuracy. In our experiment, we set λ around $1/\alpha$. In the COL-BI and the reoptimization phase, we call the simplex method from the corresponding commercial solver repeatedly. For example, We use CNET(GUROBI), noting that the simplex method is called from GUROBI, to compare with the crossover in GUROBI so that the comparison is fair. We also unified the pricing strategy in all the simplex methods we called.

Tables 1 and 2 show the comparison of the crossover results under high and low interior point precision respectively. These results demonstrate some interesting phenomenon. On the one hand, TNET and CNET both accelerate crossover solution significantly, especially when solving larger problems. Surprisingly, there is also a distinct reduction on the iteration number of the simplex using in CNET/TNET. Since it costs much less time each iteration to solve small-scale sub-problems, CNET/TNET can be very efficient. On the other hand, when the precision of the starting interior point solution is high, TNET has more obvious advantages, but its advantage over CNET is narrowed at lower precision. This maybe explained by the fact that TNET can build a BFS quite close to the optimal BFS when given a high-precision solution. However, when combining with first-order methods, which may produce very imprecise solutions, CNET may have better performance and beat TNET in turn.

Table 3 compares total run-time between different algorithms and indicates that SINKHORN+CNET is the fastest one among them. It should also be mentioned that Dong

Table 1 Crossover procedure comparison of Gurobi, CNET(Gurobi) and TNET(Gurobi) on optimal transport problems generated from MNIST dataset. The primal dual gap of the interior point solution is set to be $1E-8$.

	α	n	m	gurBarr	gurCross		CNET		TNET	
					time	iter	time	iter ¹	time	iter ²
1	1	135	180	0.41 s	0.71 s	2753	0.28 s	776	0.32 s	291
2	1	176	157	1.79 s	0.64 s	2345	0.60 s	941	0.28 s	642
3	1	113	176	0.90 s	0.27 s	2475	0.20 s	568	0.21 s	495
4	2	664	580	1.81 s	0.25 s	17312	0.64 s	4712	0.71 s	2994
5	2	768	896	3.05 s	0.60 s	46498	0.86 s	9291	0.82 s	2119
6	2	608	592	1.67 s	0.34 s	36052	1.05 s	7614	0.96 s	1615
7	3	1584	2034	17.76 s	1.74 s	76242	2.44 s	21955	1.85 s	8411
8	3	1629	1296	11.09 s	0.50 s	92954	3.45 s	30491	2.02 s	11723
9	3	1413	1053	7.10 s	0.48 s	50176	1.53 s	10210	1.58 s	7117
10	4	1040	1488	7.40 s	0.12 s	59311	1.58 s	16689	1.22 s	6862
11	4	1440	3616	24.86 s	32.06 s	140455	8.95 s	57859	3.21 s	9852
12	4	2576	2128	29.86 s	9.09 s	117379	4.05 s	37247	3.46 s	11238
13	5	4875	4500	233.28 s	215.84 s	142298	43.82 s	168182	17.65 s	33086
14	5	3275	2750	43.02 s	105.77 s	177374	48.68 s	148216	8.76 s	21634
15	5	4875	4175	184.96 s	246.66 s	146801	24.38 s	90541	15.85 s	23418

¹ The total number of the simplex iterations cost in COL-BI and reoptimization (same in Table 2)

² The total number of the simplex iterations cost in reoptimization (same in Table 2)

Table 2 Crossover procedure comparison of Gurobi, CNET(Gurobi) and TNET(Gurobi) on optimal transport problems generated from MNIST dataset. The primal dual gap of the interior point solution is set to be $1E-2$.

	α	n	m	gurBarr	gurCross		CNET		TNET	
					time	iter	time	iter	time	iter
1	1	131	110	0.88 s	0.33 s	2650	1.25 s	861	1.26 s	634
2	1	52	170	0.39 s	0.26 s	2151	0.17 s	385	0.18 s	221
3	1	172	121	0.45 s	0.20 s	3558	0.20 s	878	0.19 s	399
4	2	536	576	1.17 s	0.24 s	21652	0.49 s	4114	0.54 s	2437
5	2	340	648	0.93 s	0.31 s	28121	0.50 s	4688	0.55 s	3199
6	2	664	428	1.22 s	0.57 s	20473	0.86 s	6433	0.56 s	2403
7	3	1710	1395	14.98 s	6.16 s	92423	6.54 s	35328	5.04 s	22532
8	3	1224	1395	6.76 s	4.06 s	51173	1.11 s	12454	1.25 s	7681
9	3	1044	1404	6.23 s	5.80 s	86021	1.42 s	18976	1.25 s	5914
10	4	3136	2608	40.28 s	51.75 s	69893	4.68 s	31732	6.47 s	7721
11	4	1536	2064	15.58 s	19.07 s	136283	5.61 s	29150	5.37 s	16738
12	4	2752	1936	18.51 s	67.67 s	143621	10.25 s	47856	4.92 s	17198
14	5	3625	5400	110.92 s	282.51 s	133366	8.58 s	81217	11.97 s	18309
15	5	4150	2675	50.52 s	142.90 s	163032	12.68 s	71483	8.01 s	27360

Table 3 Total run-time comparison of Gurobi’s simplex method, Gurobi’s barrier method, Cplex’s network simplex method, Sinkhorn+CNET(Cplex), and Sinkhorn+TNET(Cplex) on optimal transport problems generated from MNIST.

	α	n	m	gurSimplex	gurBarrier	cplNetSplx	Skh+CNET	Skh+TNET
1	1	158	164	0.19 s	1.10 s	0.05 s	0.17 s	0.26 s
2	1	203	115	0.35 s	1.17 s	0.05 s	0.06 s	0.07 s
3	1	168	131	0.33 s	1.28 s	0.06 s	0.05 s	0.07 s
4	2	760	572	4.20 s	2.28 s	0.23 s	0.21 s	0.36 s
5	2	800	796	9.29 s	3.12 s	0.36 s	0.25 s	0.44 s
6	2	348	404	0.54 s	1.29 s	0.09 s	0.08 s	0.13 s
7	3	819	1494	32.04 s	6.17 s	0.67 s	0.44 s	0.81 s
8	3	1332	1278	141.20 s	9.10 s	1.13 s	0.64 s	1.03 s
9	3	2025	1386	247.53 s	16.28 s	1.98 s	1.32 s	2.46 s
10	4	832	2720	98.81 s	11.25 s	1.56 s	1.23 s	2.02 s
11	4	1968	3104	997.06 s	51.23 s	5.05 s	2.39 s	4.43 s
12	4	2752	1936	t ¹	123.42 s	4.89 s	3.19 s	5.33 s
13	5	3350	3600	t	280.12 s	10.50 s	7.73 s	15.14 s
14	5	2125	4050	t	177.75 s	6.53 s	5.26 s	11.74 s
15	5	4150	2675	t	245.74 s	14.16 s	5.21 s	8.58 s
16	6	5688	5904	t	862.93 s	48.20 s	11.03 s	30.59 s
17	6	7308	4140	t	823.22 s	56.16 s	21.87 s	37.57 s
18	6	6048	4716	t	536.69 s	42.94 s	12.20 s	27.46 s

¹ Time limit exceeded (over 1000 seconds);

et al. (2020) demonstrates that the network simplex method has the best computation performance among several exact methods via some experiments. However, SINKHORN+CNET and SINKHORN+TNET can also outperform the network simplex algorithm, especially in large-scale cases. This fully proves the power of the combination of a first-order algorithm and a good crossover algorithm.

MCF benchmark problems. As we mentioned, we implemented CNET for general MCF problems and it turns out to be also very effective. We conduct our experiments on benchmark problems from: 1) Hans Mittelmann’s large network-LP benchmark, and 2) networks generated by GOTO.

The large network-LP benchmark in Hans Mittelmann’s homepage is a set of difficult problems used to test the performance of solvers. Figure 3 shows that on this dataset, the crossover solution can be generally promoted using CNET. The right part of the figure also reveals that under different starting interior point precision, CNET is not only faster, but

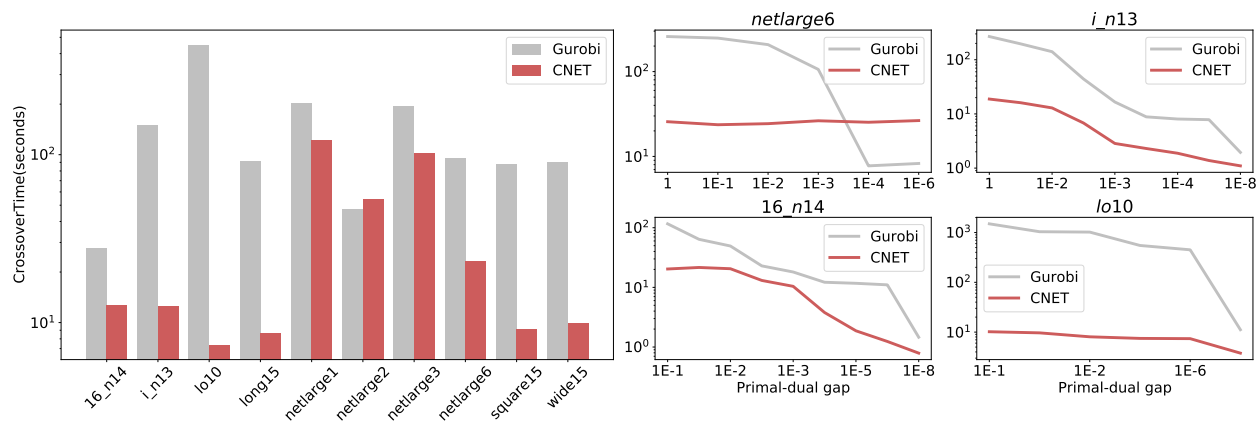


Figure 3 Computation time of crossover on the large network-LP benchmark problems. The histogram on the left shows the crossover time of different problems. The primal-dual gap of the interior point solution is set to be $1E-2$. The four line graphs on the right shows the change of the crossover run-time with the primal-dual gap of the initial interior point solution using four typical problems. The simplex method in Col-BI and the reoptimization phase is called from Gurobi (same in figure 4).

also more stable and insusceptible. This characteristic ensures the applicability of CNET for starting from the low-precision first-order solutions.

GOTO (Grid On Torus) is a well-known creator of MCF problems designed to generate hard instances (Kovács 2015)⁵. We perform experiments on this dataset to mainly test the impact of problem scale on the algorithm. It contains two types of instances: a) *GOTO_8*: sparse network: $m = 8n$; b) *GOTO_sr*: dense network: $m \approx n\sqrt{n}$, where m, n are the number of arcs and nodes in the network respectively. Figure 4 demonstrates that although the advantage of CNET reflected on run-time is heavily affected by problem scale and implementation, this advantage reflected on iteration number is quite clear and stable. And when the network becomes denser and thus usually harder to do crossover, CNET has a significant advantage. Table 4 and 5 give the specific data for *GOTO_8* and *GOTO_sr* respectively. Due to the page limit we only choose one among instances with the same network scale. Readers can find the complete table in the appendix.

5.2. Perturbation Crossover Method.

The perturbation crossover is aimed at accelerating the crossover procedure for general LP problems. In this subsection, we conduct experiments on Hans Mittelmann’s Benchmark problems for barrier LP solvers and compare with state-of-the-art commercial solvers CPLEX

⁵ We note that large-scale GOTO instances have been included in Hans Mittelmann’s large network-LP benchmark, indicating its difficulty.

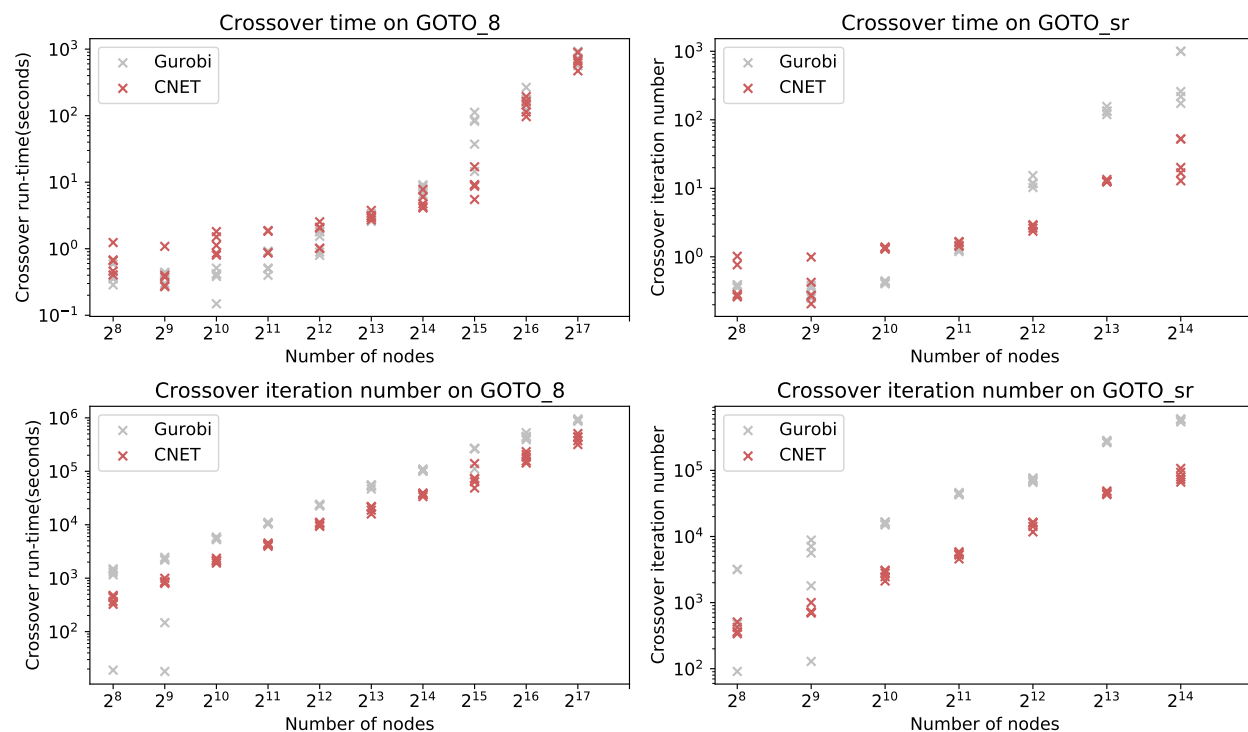


Figure 4 Computation time and iteration number of crossover on GOTO.8 and GOTO_sr. The primal-dual gap of the interior point solution is set to be $1E-2$. The iteration number of Gurobi indicates the iteration in crossover method (push phase and re-optimization) and the iteration number of CNET is the total number of the simplex steps, i.e. the total amount of iterations of Col-BI and reoptimization. 5 parallel instances are computed under each problem scale. Partial data results can be viewed in Table 4 and 5. See Table 8 and 9 in the appendix for full results.

Table 4 Computation time and iteration number of crossover on GOTO.8, corresponding to the two subfigures on the left in Figure 4 (See the complete table in the appendix)

prob	node	arc	ratio	gurBarr	Gurobi		CNET	
					time	iteration	time	iteration
8.08a	256	2048	8	0.55 s	0.41 s	1497	0.68 s	436
8.09a	512	4096	8	0.72 s	0.41 s	147	0.27 s	799
8.10a	1024	8192	8	1.25 s	0.41 s	5897	0.86 s	2362
8.11a	2048	16384	8	2.49 s	0.40 s	10445	0.87 s	4193
8.12a	4096	32768	8	1.45 s	0.89 s	22477	1.01 s	9669
8.13a	8192	65536	8	4.74 s	3.07 s	56060	2.71 s	21669
8.14a	16384	131072	8	8.26 s	8.69 s	108819	4.10 s	36804
8.15a	32768	262144	8	230.31 s	14.51 s	111110	5.49 s	48676
8.16a	65536	524288	8	90.60 s	159.54 s	418446	113.38 s	155959
8.17a	131072	1048576	8	213.63 s	564.17 s	864135	471.25 s	316871

and MOSEK⁶, showing that the underlying crossover method can work on all LP solvers.

⁶ We do not put GUROBI because it does not have the appropriate interface for warming starting simplex method from given solutions. Most commercial solvers have the interface for warm starting from given basis information or given

Table 5 Computation time and iteration number of crossover on GOTO_sr, corresponding to the two subfigures on the right in Figure 4 (See the complete table in the appendix)

prob	node	arc	ratio	gurBarr	Gurobi		CNET	
					time	iteration	time	iteration
sr_08a	256	4096	16	0.82 s	0.38 s	91	0.27 s	338
sr_09a	512	11585	22.63	0.60 s	0.28 s	8844	0.42 s	724
sr_10a	1024	32768	32	0.75 s	0.45 s	16461	1.39 s	2985
sr_11a	2048	92682	45.25	1.13 s	1.19 s	43540	1.42 s	5647
sr_12a	4096	262144	64	5.64 s	10.28 s	68923	2.37 s	14208
sr_13a	8192	741455	90.51	32.46 s	133.95 s	269178	12.83 s	43411
sr_14a	16384	2097152	128	94.83 s	t ¹	-	52.23 s	93377
sr_15a	32768	5931642	181.02	982.65 s	t	-	261.89 s	178643

¹ Time limit exceeded (over 1000 seconds);

In our experiments, the presolve phase in all solvers is turned off, in order to make the crossover comparison fairer.

Since the perturbation crossover method is especially valuable for the problem with a high-dimension optimal face, it might not have a good performance in accelerating the problems whose crossover procedure is already fast enough. Therefore, we consider the problems whose crossover procedure is a bottleneck for designing an efficient barrier algorithm. In other word, even when starting from an approximate solution with high accuracy, it still takes a long time to find a vertex solution. In this section, we chose all the problems whose crossover time is at least five times longer than the barrier method time to study. More results can be referred to in the appendix

In the solution process using the perturbation method, we start with an interior point solution and construct a perturbed problem based on section 4. Then we call the barrier algorithm without a crossover stage to solve this perturbed problem. The next step differs between CPLEX and MOSEK. In experiments with CPLEX, we can feed the interior point solution to the crossover interface leading to the original problem directly. The MOSEK, however, has no such interface of crossover, thus we have to run the crossover stage continuously on the perturbed problem and then feed the BFS returned to the Simplex method solving the original problem.

Table 6 compares the original crossover procedure of CPLEX and our perturbation crossover method by starting from the same default interior point solution. It shows that

solutions. Unlike MCF problems where we can get exact basis information from the basis identification phase, for general LPs, the barrier algorithm solvers may not output the basis information so we let all solvers warm start from given solutions, which is supposed to be equivalent to providing a starting basis. However in our experiments GUROBI doesn't benefit from the given solutions at all and spends the same time as no warm starting.

Table 6 Cplex’s computation time on the barrier LP benchmark problems with long crossover time.

	problem	cplBarr	original		perturbed	
			cplCross ¹	cplBarr ²	cplCross ³	total
1	graph40-40	0.69 s	92.89 s	9.92 s	35.52 s	45.44 s
2	datt256	3.49 s	284.44 s	3.20 s	20.50 s	23.70 s
3	nug08-3rd	1.25 s	88.75 s	0.03 s	64.73 s	64.77 s
4	cont11	7.24 s	221.69 s	8.36 s	271.25 s	279.61 s
5	cont1	2.50 s	70.41 s	1.66 s	62.58 s	64.23 s
6	shs1023	15.42 s	365.36 s	16.47 s	281.81 s	298.28 s
7	savsched1	7.64 s	108.45 s	10.39 s	14.64 s	25.03 s
8	chrom1024-7	0.20 s	2.63 s	1.41 s	1.09 s	2.50 s
9	neos3	1.45 s	15.48 s	6.75 s	67.05 s	73.80 s
10	fhnw-bin0	1.53 s	12.84 s	9.98 s	10.77 s	20.75 s
11	self	0.99 s	5.87 s	0.70 s	2.67 s	3.38 s
12	qap15	0.39 s	2.06 s	1.45 s	1.58 s	3.03 s

¹ CPLEX’s crossover method after the barrier on the original problem;

² CPLEX’s barrier algorithm without crossover on the perturbed problem;

³ CPLEX’s crossover method on the original problem using the solution of cplBarr;

Table 7 Mosek’s computation time on the barrier LP benchmark problems with long crossover time.

	problem	mskBarr	original		perturbed		
			mskCross ¹	mskBarr ²	mskCross ³	mskSplx ⁴	total
1	datt256	3.61 s	349.36 s	4.50 s	4.13 s	1.45 s	10.08 s
2	ns1688926	3.53 s	87.55 s	3.03 s	87.52 s	0.31 s	90.86 s
3	stat96v1	9.20 s	104.72 s	0.33 s	0.30 s	65.36 s	65.99 s
4	graph40-40	18.20 s	158.17 s	30.08 s	6.45 s	0.58 s	37.11 s
5	savsched1	17.19 s	113.30 s	42.45 s	5.41 s	0.88 s	48.73 s
6	self	1.02 s	5.80 s	1.11 s	0.19 s	0.14 s	1.44 s

¹ MOSEK’s crossover method after the barrier on the original problem;

² MOSEK’s barrier algorithm without crossover on the perturbed problem;

³ MOSEK’s crossover method after the barrier on the perturbed problem;

⁴ MOSEK’s simplex method on the original problem when warmly starting with the solution of mskCross;

our perturbation crossover makes a significant improvement and thoroughly removes the bottleneck for some problems. For example, the crossover for *datt256_lp* is a common bottleneck for almost all commercial LP solvers⁷, since the barrier algorithm can terminate usually in no more than 4 seconds while the crossover procedure takes a much longer time. However, our perturbation crossover can perfectly solve it. Table 7 demonstrates the results on MOSEK. It is worth noting that there is one more step in the perturbation method due

⁷ <http://plato.asu.edu/ftp/lpbar.html> (Accessed: 14 August, 2021)

to our previous explanation. And although one more extra step is needed, the perturbation is still powerful.

Moreover, in the practical computation, some typical features can be extracted to determine whether to perturb the original problem or not. These features include: the number of iteration in the barrier algorithm, the sparsity of the A -matrix, and the number of variables that need to be pushed. Again, as we mentioned, the success of perturbation on COPT can prove its practical feasibility. Also note that, dependent on the size of perturbation, there exists a balance between the crossover computation time of the perturbed feasibility problem and that of the reoptimization phase, so in practice solvers can benefit from the perturbation crossover method by concurrently running both the traditional crossover and our perturbation crossover with different size of perturbation to be more robust.

Acknowledgments

We thank Fangkun Qiu for fruitful discussions and some valuable experiments.

References

- Ahuja RK, Orlin JB, Magnanti TL (1993) *Network flows: theory, algorithms, and applications* (Prentice Hall).
- Altschuler J, Weed J, Rigollet P (2017) Near-linear time approximation algorithms for optimal transport via Sinkhorn iteration. *Advances in Neural Information Processing Systems* 30, 1961—1971.
- Andersen ED (1999) On exploiting problem structure in a basis identification procedure for linear programming. *INFORMS Journal on Computing* 11(1):95–103.
- Andersen ED, Ye Y (1996) Combining interior-point and pivoting algorithms for linear programming. *Management Science* 42(12):1719–1731.
- Applegate D, Díaz M, Hinder O, Lu H, Lubin M, O’Donoghue B, Schudy W (2021a) Practical large-scale linear programming using primal-dual hybrid gradient. *Advances in Neural Information Processing Systems* 34:20243–20257.
- Applegate D, Hinder O, Lu H, Lubin M (2021b) Faster first-order primal-dual methods for linear programming using restarts and sharpness. *arXiv preprint arXiv:2105.12715* .
- Benamou JD, Carlier G, Cuturi M, Nenna L, Peyré G (2015) Iterative bregman projections for regularized transportation problems. *SIAM Journal on Scientific Computing* 37(2):A1111–A1138.
- Bertsekas DP, Castanon DA (1989) The auction algorithm for the transportation problem. *Annals of Operations Research* 20(1):67–96.
- Bertsimas D, Tsitsiklis JN (1997) *Introduction to linear optimization* (Athena Scientific Belmont, MA).
- Bixby RE, Saltzman MJ (1994) Recovering an optimal LP basis from an interior point solution. *Operations Research Letters* 15(4):169–178.
- Bowman EH (1956) Production scheduling by the transportation method of linear programming. *Operations Research* 4(1):100–103.
- Buttazzo G, De Pascale L, Gori-Giorgi P (2012) Optimal-transport formulation of electronic density-functional theory. *Physical Review A* 85(6):062502.
- Carlier G, Ekeland I (2010) Matching for teams. *Economic theory* 42(2):397–418.
- Charnes A, Cooper WW (1954) The stepping stone method of explaining linear programming calculations in transportation problems. *Management Science* 1(1):49–69.
- Chazelle B (2000) A minimum spanning tree algorithm with inverse-Ackermann type complexity. *Journal of the ACM (JACM)* 47(6):1028–1047.
- Cotar C, Friesecke G, Klüppelberg C (2013) Density functional theory and optimal transportation with Coulomb cost. *Communications on Pure and Applied Mathematics* 66(4):548–599.
- Cuturi M (2013) Sinkhorn distances: Lightspeed computation of optimal transport. *Advances in Neural Information Processing Systems* 26, 2292–2300.

- Cuturi M, Doucet A (2014) Fast computation of Wasserstein barycenters. *Proceedings of the 31st International Conference on Machine Learning*, 685–693.
- Dantzig GB (1963) *Linear programming and extensions* (Princeton University Press).
- Dijkstra EW, et al. (1959) A note on two problems in connexion with graphs. *Numerische Mathematik* 1(1):269–271.
- Dong Y, Gao Y, Peng R, Razenshteyn I, Sawlani S (2020) A study of performance of optimal transport. *arXiv preprint arXiv:2005.01182* .
- Dvurechensky P, Gasnikov A, Kroshnin A (2018) Computational optimal transport: Complexity by accelerated gradient descent is better than by Sinkhorn’s algorithm. *Proceedings of the 35th International Conference on Machine Learning*, 1367–1376.
- Galabova I, Hall J (2020) The ‘Idiot’ crash quadratic penalty algorithm for linear programming and its application to linearizations of quadratic assignment problems. *Optimization Methods and Software* 35(3):488–501.
- Galichon A (2018) *Optimal transport methods in economics* (Princeton University Press).
- Gao W, Sun C, Ye Y, Ye Y (2021) Boosting method in approximately solving linear programming with fast online algorithm. *arXiv preprint arXiv:2107.03570* .
- Ge D, Wang H, Xiong Z, Ye Y (2019) Interior-point methods strike back: solving the Wasserstein barycenter problem. *Advances in Neural Information Processing Systems 32*, 6894–6905.
- Genevay A, Cuturi M, Peyré G, Bach F (2016) Stochastic optimization for large-scale optimal transport. *Advances in Neural Information Processing Systems 29*, 3440–3448.
- Goldman AJ, Tucker AW (1956) Theory of linear programming. *Linear Inequalities and Related Systems* 38:53–97.
- Güler O, Ye Y (1993) Convergence behavior of interior-point algorithms. *Mathematical Programming* 60(1-3):215–228.
- Hanssmann F, Hess SW (1960) A linear programming approach to production and employment scheduling. *Management Science* MT-1(1):46–51.
- Ho N, Huynh V, Phung D, Jordan M (2019) Probabilistic multilevel clustering via composite transportation distance. *The 22nd International Conference on Artificial Intelligence and Statistics*, 3149–3157.
- Jambulapati A, Sidford A, Tian K (2019) A direct $\tilde{o}(1/\epsilon)$ iteration parallel algorithm for optimal transport. *Advances in Neural Information Processing Systems 32*, 11359–11370.
- Janati H, Cuturi M, Gramfort A (2020) Debaised Sinkhorn barycenters. *Proceedings of the 37th International Conference on Machine Learning*, 4692–4701.
- Karger DR, Klein PN, Tarjan RE (1995) A randomized linear-time algorithm to find minimum spanning trees. *Journal of the ACM (JACM)* 42(2):321–328.

- Klee V, Minty GJ (1972) How good is the simplex algorithm. *Inequalities* 3(3):159–175.
- Kojima M, Mizuno S, Yoshise A (1989) A polynomial-time algorithm for a class of linear complementarity problems. *Mathematical Programming* 44(1-3):1–26.
- Kortanek K, Jishan Z (1988) New purification algorithms for linear programming. *Naval Research Logistics (NRL)* 35(4):571–583.
- Kovács P (2015) Minimum-cost flow algorithms: an experimental evaluation. *Optimization Methods and Software* 30(1):94–127.
- Kroshnin A, Tupitsa N, Dvinskikh D, Dvurechensky P, Gasnikov A, Uribe C (2019) On the complexity of approximating Wasserstein barycenters. *Proceedings of the 36th International Conference on Machine Learning*, 3530–3540.
- Kruskal JB (1956) On the shortest spanning subtree of a graph and the traveling salesman problem. *Proceedings of the American Mathematical Society* 7(1):48–50.
- Li X, Sun D, Toh KC (2020) An asymptotically superlinearly convergent semismooth Newton augmented Lagrangian method for linear programming. *SIAM Journal on Optimization* 30(3):2410–2440.
- Lin T, Ho N, Chen X, Cuturi M, Jordan MI (2020a) Fixed-support Wasserstein barycenters: computational hardness and fast algorithm. *Advances in Neural Information Processing Systems 33 Pre-proceedings*.
- Lin T, Ho N, Jordan MI (2019) On the efficiency of the Sinkhorn and Greenhorn algorithms and their acceleration for optimal transport. *The 36th International Conference on Artificial Intelligence and Statistics*, 3982–3991.
- Lin T, Ma S, Ye Y, Zhang S (2020b) An ADMM-based interior-point method for large-scale linear programming. *Optimization Methods and Software* 0(0):1–36.
- Liu Q, Van Ryzin G (2008) On the choice-based linear programming model for network revenue management. *Manufacturing & Service Operations Management* 10(2):288–310.
- Liu XW, Dai YH, Huang YK (2022) A primal-dual majorization-minimization method for large-scale linear programs. *arXiv preprint arXiv:2208.03672* .
- Megiddo N (1991) On finding primal-and dual-optimal bases. *ORSA Journal on Computing* 3(1):63–65.
- Mehrotra S, Ye Y (1993) Finding an interior point in the optimal face of linear programs. *Mathematical Programming* 62(1-3):497–515.
- Mitra G, Tamiz M, Yadegar J (1988) Experimental investigation of an interior search method within a simplex framework. *Communications of the ACM* 31(12):1474–1482.
- Nguyen X (2013) Convergence of latent mixing measures in finite and infinite mixture models. *The Annals of Statistics* 41(1):370–400.
- O’donoghue B, Chu E, Parikh N, Boyd S (2016) Conic optimization via operator splitting and homogeneous self-dual embedding. *Journal of Optimization Theory and Applications* 169(3):1042–1068.

- Prim RC (1957) Shortest connection networks and some generalizations. *The Bell System Technical Journal* 36(6):1389–1401.
- Santambrogio F (2015) *Optimal transport for applied mathematicians* (Springer).
- Skajaa A, Andersen ED, Ye Y (2013) Warmstarting the homogeneous and self-dual interior point method for linear and conic quadratic problems. *Mathematical Programming Computation* 5(1):1–25.
- Villani C (2003) *Topics in optimal transportation* (American Mathematical Society).
- Wagner HM (1959) On a class of capacitated transportation problems. *Management Science* 5(3):304–318.
- Yang L, Li J, Sun D, Toh KC (2021) A fast globally linearly convergent algorithm for the computation of Wasserstein barycenters. *The Journal of Machine Learning Research* 22(1):984–1020.
- Ye Y (1992) On the finite convergence of interior-point algorithms for linear programming. *Mathematical Programming* 57(1-3):325–335.
- Yildirim EA, Wright SJ (2002) Warm-start strategies in interior-point methods for linear programming. *SIAM Journal on Optimization* 12(3):782–810.

Appendix A: Proof of Lemma 1

Proof of Lemma 1 We can shift the problem (11) to construct an equivalent MCF problem. The new MCF problem is based on the network $\bar{\mathcal{G}} := (\bar{\mathcal{N}}, \bar{\mathcal{A}})$, in which

$$\bar{\mathcal{N}} = \mathcal{N}, \quad \bar{\mathcal{A}} = \mathcal{L} \cup \{(j, i) : (i, j) \in \mathcal{U}\}. \quad (22)$$

Accordingly, the capacity limit \bar{u} remains the same in the corresponding modified arcs; and the cost \bar{c} in the same direction remain unchanged but cost in the opposite direction turns opposite. i.e.,

$$\begin{aligned} \bar{u}_{\mathcal{L}} &= u_{\mathcal{L}} \text{ and } \bar{u}_{ji} = u_{ij} \text{ when } (i, j) \in \mathcal{U} \\ \bar{c}_{\mathcal{L}} &= c_{\mathcal{L}} \text{ but } \bar{c}_{ji} = -c_{ij} \text{ when } (i, j) \in \mathcal{U} \end{aligned} \quad (23)$$

Given any flow f in the original problem (11), we can construct the corresponding new flow \bar{f} by

$$\bar{f}_{ij} = \begin{cases} f_{ij} & 0 \leq f_{ij} \leq u_{ij} \text{ and } (i, j) \in \mathcal{L} \\ u_{ij} - f_{ij} & 0 \leq f_{ij} \leq u_{ij} \text{ and } (i, j) \in \mathcal{U} \end{cases} \quad (24)$$

And $\bar{b}_i = b_i - \sum_{(i,j) \in \mathcal{U}} u_{ij} + \sum_{(j,i) \in \mathcal{U}} u_{ij}$. Then, the new MCF problem $MCF(\bar{f})$ is as follows:

$$\begin{aligned} \min_f & \sum_{(i,j) \in \bar{\mathcal{A}}} \bar{c}_{ij} \bar{f}_{ij} \\ \text{s. t.} & \bar{b}_i + \sum_{j \in I(i)} \bar{f}_{ji} = \sum_{j \in O(i)} \bar{f}_{ij}, \quad \forall i \in \bar{\mathcal{N}} \\ & 0 \leq \bar{f}_{ij} \leq \bar{u}_{ij}, \quad \forall (i, j) \in \bar{\mathcal{A}} \end{aligned} \quad (25)$$

Now easy to see that now \bar{f} is feasible for the new problem $MCF(\bar{b}, \bar{c}, \bar{u})$ if and only if f is feasible for the original problem $MCF(b, c, u)$.

Besides, we have

$$\sum_{(i,j) \in \bar{\mathcal{A}}} \bar{c}_{ij} \bar{f}_{ij} = \sum_{(i,j) \in \mathcal{A}} c_{ij} f_{ij} - \sum_{(j,i) \in \mathcal{U}} c_{ji} u_{ji}.$$

Therefore, \bar{f} is an optimal solution for the problem $MCF(\bar{b}, \bar{c}, \bar{u})$ if and only if f is an optimal solution for the original problem $MCF(b, c, f)$. \square

Appendix B: Complete Table of Numerical Experiments

We here show the complete version of Table 4, 5, 6 and 7.

Table 8 Computation time and iteration number of crossover on GOTO_8 (complete table)

prob	node	arc	ratio	gurBarr	Gurobi		CNET	
					time	iteration	time	iteration
8_08a	256	2048	8	0.55 s	0.41 s	1497	0.68 s	436
8_08b	256	2048	8	0.83 s	0.35 s	19	0.46 s	324
8_08c	256	2048	8	1.25 s	0.59 s	1288	1.24 s	463
8_08d	256	2048	8	1.38 s	0.38 s	1158	0.40 s	367
8_08e	256	2048	8	0.70 s	0.29 s	1401	0.66 s	476
8_09a	512	4096	8	0.72 s	0.41 s	147	0.27 s	799
8_09b	512	4096	8	1.12 s	0.40 s	2456	1.08 s	997
8_09c	512	4096	8	1.19 s	0.44 s	2176	0.40 s	830
8_09d	512	4096	8	1.21 s	0.43 s	2319	0.37 s	834
8_09e	512	4096	8	0.91 s	0.30 s	18	0.28 s	866
8_10a	1024	8192	8	1.25 s	0.41 s	5897	0.86 s	2362
8_10b	1024	8192	8	1.93 s	0.51 s	5580	1.12 s	2072
8_10c	1024	8192	8	2.57 s	0.42 s	5369	1.51 s	1914
8_10d	1024	8192	8	4.03 s	0.15 s	5273	1.81 s	2115
8_10e	1024	8192	8	1.40 s	0.38 s	5461	0.80 s	2174
8_11a	2048	16384	8	2.49 s	0.40 s	10445	0.87 s	4193
8_11b	2048	16384	8	4.88 s	0.51 s	10733	1.87 s	4549
8_11c	2048	16384	8	4.25 s	0.92 s	11095	1.84 s	4255
8_11d	2048	16384	8	4.56 s	0.89 s	10728	1.84 s	4315
8_11e	2048	16384	8	1.80 s	0.50 s	10304	0.87 s	3958
8_12a	4096	32768	8	1.45 s	0.89 s	22477	1.01 s	9669
8_12b	4096	32768	8	2.91 s	1.54 s	23485	2.10 s	10725
8_12c	4096	32768	8	2.64 s	1.79 s	24133	2.05 s	10562
8_12d	4096	32768	8	2.83 s	1.82 s	23567	2.54 s	11133
8_12e	4096	32768	8	1.52 s	0.80 s	22957	1.02 s	9342
8_13a	8192	65536	8	4.74 s	3.07 s	56060	2.71 s	21669
8_13b	8192	65536	8	8.68 s	3.37 s	53125	3.13 s	18745
8_13c	8192	65536	8	9.21 s	2.58 s	46638	2.91 s	15910
8_13d	8192	65536	8	7.88 s	3.25 s	54287	3.76 s	21281
8_13e	8192	65536	8	4.00 s	2.90 s	53062	3.09 s	21894
8_14a	16384	131072	8	8.26 s	8.69 s	108819	4.10 s	36804
8_14b	16384	131072	8	17.81 s	9.14 s	109988	7.77 s	39385
8_14c	16384	131072	8	14.73 s	6.59 s	101479	4.74 s	36211
8_14d	16384	131072	8	7.58 s	7.46 s	99774	4.31 s	33571
8_14e	16384	131072	8	9.51 s	7.94 s	103135	6.02 s	37337
8_15a	32768	262144	8	230.31 s	14.51 s	111110	5.49 s	48676
8_15b	32768	262144	8	174.41 s	82.46 s	265717	8.69 s	71309
8_15c	32768	262144	8	221.29 s	86.70 s	266790	9.17 s	74090
8_15d	32768	262144	8	164.17 s	37.34 s	264769	9.13 s	63589
8_15e	32768	262144	8	214.60 s	112.48 s	267788	17.03 s	139645
8_16a	65536	524288	8	90.60 s	159.54 s	418446	113.38 s	155959
8_16b	65536	524288	8	78.00 s	123.47 s	390564	96.76 s	142624
8_16c	65536	524288	8	69.36 s	177.45 s	451769	164.25 s	205164
8_16d	65536	524288	8	74.44 s	170.31 s	432678	145.61 s	183577
8_16e	65536	524288	8	46.33 s	265.79 s	526544	193.55 s	233477
8_17a	131072	1048576	8	213.63 s	564.17 s	864135	471.25 s	316871
8_17b	131072	1048576	8	205.18 s	732.09 s	900614	700.48 s	443627
8_17c	131072	1048576	8	175.34 s	705.82 s	887913	618.93 s	373501
8_17d	131072	1048576	8	184.19 s	868.57 s	921300	659.82 s	434467
8_17e	131072	1048576	8	175.48 s	928.17 s	955180	896.46 s	508843

Table 9 Computation time and iteration number of crossover on GOTO_sr (complete table)

prob	node	arc	ratio	gurBarr	Gurobi		CNET	
					time	iteration	time	iteration
sr_08a	256	4096	16	0.82 s	0.38 s	91	0.27 s	338
sr_08b	256	4096	16	0.78 s	0.38 s	497	0.28 s	353
sr_08c	256	4096	16	0.79 s	0.36 s	475	0.26 s	364
sr_08d	256	4096	16	0.67 s	0.39 s	3175	0.77 s	422
sr_08e	256	4096	16	0.70 s	0.36 s	3181	1.02 s	510
sr_09a	512	11585	22.63	0.60 s	0.28 s	8844	0.42 s	724
sr_09b	512	11585	22.63	0.84 s	0.36 s	1796	0.27 s	712
sr_09c	512	11585	22.63	0.86 s	0.35 s	129	0.27 s	696
sr_09d	512	11585	22.63	0.78 s	0.38 s	7074	0.99 s	1003
sr_09e	512	11585	22.63	0.67 s	0.25 s	5633	0.21 s	718
sr_10a	1024	32768	32	0.75 s	0.45 s	16461	1.39 s	2985
sr_10b	1024	32768	32	0.76 s	0.40 s	16515	1.32 s	2467
sr_10c	1024	32768	32	0.84 s	0.42 s	15491	1.30 s	2792
sr_10d	1024	32768	32	0.77 s	0.42 s	16452	1.31 s	2122
sr_10e	1024	32768	32	0.83 s	0.42 s	14965	1.36 s	3092
sr_11a	2048	92682	45.25	1.13 s	1.19 s	43540	1.42 s	5647
sr_11b	2048	92682	45.25	1.41 s	1.25 s	44279	1.65 s	5247
sr_11c	2048	92682	45.25	1.22 s	1.28 s	44446	1.67 s	5361
sr_11d	2048	92682	45.25	1.38 s	1.26 s	42735	1.63 s	5875
sr_11e	2048	92682	45.25	1.23 s	1.41 s	46224	1.47 s	4580
sr_12a	4096	262144	64	5.64 s	10.28 s	68923	2.37 s	14208
sr_12b	4096	262144	64	8.09 s	11.75 s	77023	2.88 s	15869
sr_12c	4096	262144	64	6.26 s	11.81 s	73286	2.87 s	16166
sr_12d	4096	262144	64	6.76 s	11.87 s	70840	2.94 s	16463
sr_12e	4096	262144	64	5.73 s	15.34 s	65709	2.62 s	11723
sr_13a	8192	741455	90.51	32.46 s	133.95 s	269178	12.83 s	43411
sr_13b	8192	741455	90.51	19.65 s	134.09 s	280913	12.75 s	48794
sr_13c	8192	741455	90.51	22.24 s	133.40 s	263402	12.38 s	43251
sr_13d	8192	741455	90.51	24.43 s	119.26 s	265464	12.45 s	44700
sr_13e	8192	741455	90.51	21.36 s	156.35 s	282448	13.46 s	46603
sr_14a	16384	2097152	128	94.83 s	t ¹	-	52.23 s	93377
sr_14b	16384	2097152	128	119.55 s	t	-	52.85 s	107051
sr_14c	16384	2097152	128	216.21 s	258.58 s	588209	12.88 s	73004
sr_14d	16384	2097152	128	231.49 s	218.55 s	570491	20.13 s	79406
sr_14e	16384	2097152	128	192.36 s	173.44 s	540502	16.83 s	66516
sr_15a	32768	5931642	181.02	982.65 s	t	-	261.89 s	178643
sr_15b	32768	5931642	181.02	1013.28 s	t	-	216.12 s	173889
sr_15c	32768	5931642	181.02	1235.67 s	t	-	204.29 s	158916
sr_15d	32768	5931642	181.02	1968.39 s	t	-	51.46 s	131593
sr_15e	32768	5931642	181.02	1096.18 s	t	-	225.66 s	177414

¹ Time limit exceeded (over 1000 seconds);

Table 10 Cplex's computation time on the barrier LP benchmark problems (complete table for problems with longer crossover time).

	problem	ratio	cplBarr	original		perturbed		total
				cplCross	cplBarr	cplCross		
1	graph40-40	135.21	0.69 s	92.89 s	9.92 s	35.52 s	45.44 s	
2	datt256	81.62	3.49 s	284.44 s	3.20 s	20.50 s	23.70 s	
3	nug08-3rd	71.00	1.25 s	88.75 s	0.03 s	64.73 s	64.77 s	
4	cont11	30.64	7.24 s	221.69 s	8.36 s	271.25 s	279.61 s	
5	cont1	28.16	2.50 s	70.41 s	1.66 s	62.58 s	64.23 s	
6	shs1023	23.69	15.42 s	365.36 s	16.47 s	281.81 s	298.28 s	
7	savshed1	14.19	7.64 s	108.45 s	10.39 s	14.64 s	25.03 s	
8	chrom1024-7	12.93	0.20 s	2.63 s	1.41 s	1.09 s	2.50 s	
9	neos3	10.66	1.45 s	15.48 s	6.75 s	67.05 s	73.80 s	
10	fhnw-bin0	8.38	1.53 s	12.84 s	9.98 s	10.77 s	20.75 s	
11	self	5.96	0.99 s	5.87 s	0.70 s	2.67 s	3.38 s	
12	qap15	5.28	0.39 s	2.06 s	1.45 s	1.58 s	3.03 s	
13	stat96v1	3.52	1.92 s	6.77 s	0.55 s	225.00 s	225.55 s	
14	square41	3.04	1.17 s	3.56 s	3.58 s	28.05 s	31.63 s	
15	ns1687037	1.65	23.94 s	39.48 s	43.64 s	t	-	
16	tp-6	1.59	41.84 s	66.44 s	12.47 s	t	-	
17	fome13	1.55	1.16 s	1.80 s	0.20 s	1.77 s	1.97 s	
18	tpl-tub-ws	1.53	32.08 s	49.11 s	12.19 s	63.20 s	75.39 s	
19	karted	1.44	25.55 s	36.72 s	8.53 s	143.77 s	152.30 s	
20	Linf_520c	1.32	7.13 s	9.42 s	13.03 s	155.99 s	169.02 s	

Table 11 Mosek's computation time on the barrier LP benchmark problems (complete table for problems with longer crossover time).

	problem	ratio	mskBarr	original		perturbed		total
				mskCross	mskBarr	mskCross	mskSplx	
1	datt256	96.78	3.61 s	349.36 s	4.50 s	4.13 s	1.45 s	10.08 s
2	ns1688926	24.79	3.53 s	87.55 s	3.03 s	87.52 s	0.31 s	90.86 s
3	stat96v1	11.38	9.20 s	104.72 s	0.33 s	0.30 s	65.36 s	65.99 s
4	graph40-40	8.69	18.20 s	158.17 s	30.08 s	6.45 s	0.58 s	37.11 s
5	savshed1	6.59	17.19 s	113.30 s	42.45 s	5.41 s	0.88 s	48.73 s
6	self	5.70	1.02 s	5.80 s	1.11 s	0.19 s	0.14 s	1.44 s
7	nug08-3rd	4.44	27.27 s	121.13 s	69.57 s	131.02 s	t	-
8	karted	3.80	6.95 s	26.42 s	0.03 s	0.02 s	t	-
9	chrom1024-7	2.82	3.39 s	9.58 s	3.78 s	0.72 s	t	-
10	fhnw-bin0	2.62	10.94 s	28.61 s	5.45 s	12.83 s	131.39 s	149.67 s
11	degme	2.33	23.70 s	55.16 s	13.82 s	1.31 s	2.72 s	17.84 s
12	tp-6	2.28	25.84 s	58.86 s	13.21 s	152.01 s	83.56 s	248.78 s
13	ts-palko	1.98	4.38 s	8.66 s	8.30 s	74.22 s	115.36 s	197.88 s
14	irish-e	1.68	57.94 s	97.39 s	3.14 s	5.52 s	6.69 s	15.34 s
15	tpl-tub-ws	1.41	167.34 s	236.33 s	51.73 s	148.41 s	t	-
16	neos3	1.36	8.45 s	11.49 s	39.82 s	160.95 s	t	-
17	fome13	1.01	10.33 s	10.42 s	1.06 s	0.50 s	71.41 s	72.97 s